Nonlinear stresses and temperatures in transient adiabatic and shear flows via nonequilibrium molecular dynamics: Three definitions of temperature

Wm. G. Hoover and C. G. Hoover
Ruby Valley Research Institute, Highway Contract 60, Box 598, Ruby Valley, 89833 Nevada, USA
(Received 12 November 2008; revised manuscript received 30 January 2009)

We compare nonlinear stresses and temperatures for adiabatic-shear flows, using up to 262 144 particles, with those from corresponding homogeneous and inhomogeneous flows. Two varieties of kinetic temperature tensors are compared to the configurational temperatures. This comparison of temperatures led us to two findings beyond our original goal of analyzing shear algorithms. First, we found an improved form for local instantaneous velocity fluctuations, as calculated with smooth-particle weighting functions. Second, we came upon the previously unrecognized contribution of rotation to the configurational temperature.

DOI: XXXX PACS number(s): 02.70.Ns, 45.10.−b, 46.15.−x, 47.11.Mn

I. INTRODUCTION

Hoover *et al.* [1] studied the nonlinear stresses and temperature changes induced by shear in a variety of stationary flows. They used nonequilibrium molecular dynamics to compare several popular algorithms. The algorithms are described briefly in Sec. II. See Figs. 1 and 2 for the geometries used to induce the flows. This work used a smooth repulsive soft-sphere potential [2] with a range of unity,

$$\phi(r<1) = 100(1-r^2)^4.$$

The particle mass, energy per particle, and density were all chosen equal to unity. These conditions correspond to a dense fluid at about 2/3 the freezing pressure,

$$m = 1; \quad E/N = (K+\Phi)/N = 1; \quad \rho = Nm/V = 1.$$

Thermostat or ergostat forces were used to generate stationary states. There, as well as in the present work, we choose x for the flow direction and $\dot{\epsilon}=0.5$ for the strain rate, where the time-averaged velocity component of the flow v_x increases linearly in the y direction,

$$\langle v_x(y)\rangle = \dot{\epsilon} y.$$

Three-dimensional homogeneous periodic simulations (Fig. 1 shows a two-dimensional version) gave

$$T_{yy} > T_{xx} > T_{zz}, \quad P_{yy} > P_{xx} > P_{zz} \text{ [Doll's algorithm]},$$

$$T_{xx} > T_{yy} > T_{zz}, \quad P_{xx} > P_{yy} > P_{zz} \text{ [Sllod algorithm]},$$

and differed qualitatively from the corresponding three-dimensional boundary-driven results (Fig. 2 shows a two-dimensional version),

$$T_{xx} > T_{zz} > T_{yy}, \quad P_{xx} > P_{zz} > P_{yy} \text{ [boundary-driven]}.$$

The main conclusion drawn from that work was that *neither* homogeneous method, Doll's [3] nor Sllod [4], successfully reproduces the more-physical boundary-driven results [5]. To quote Ref. [1] "the Doll's and Sllod algorithms predict opposite signs for this normal-stress difference $[P_{xx}-P_{yy}]$, with the Sllod approach definitely wrong, but somewhat closer to the (boundary-driven) truth."

Evans [6] objected to this conclusion, stating that the Sllod algorithm is "exact." He is of course correct, in the sense that the Sllod algorithm is nothing more than Newton's equations of motion written in a different coordinate frame, a Lagrangian frame moving along with the sheared fluid. But because Newton's equations by themselves cannot lead to nonequilibrium steady states, the Sllod algorithm is exact in the rather limited case of isolated systems.

The misunderstanding evident in Evans' remark led us to undertake the present work. Instead of considering steady states, which seem to us the simplest situation, Evans had in mind a time-dependent spatially periodic adiabatic deformation. When no thermostat or ergostat forces are used in the equations of motion, the shear deformation is adiabatic with continuous heating. In the adiabatic case no steady state results and the Sllod equations of motion are equivalent to Newton's equations of motion for a system undergoing periodic deformation with strain rate $\dot{\epsilon}$. Just as in the thermostated case the normal stresses and temperatures differ. Not only the magnitudes but also the orderings of these components can, and do, differ from those found in steady states.

In this paper we motivate and describe large-scale adiabatic-shear simulations and discuss the interpretation of these simulations. These simulations use periodic boundary

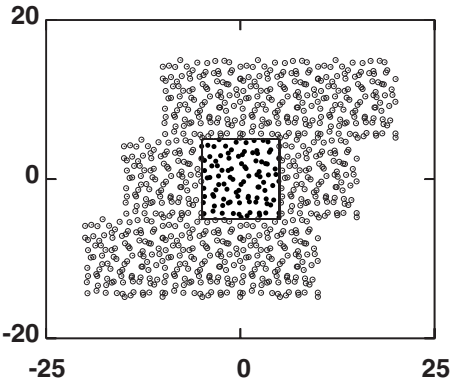

FIG. 1. Two-dimensional version of periodic homogeneous isoenergetic shear flow. Eight periodic images of the central N-particle system are shown. In this figure, as in all the others, the units are dimensionless, where the volume per particle, the particle mass, and Boltzmann's constant k are all equal to unity. Thus the plotted lengths, times, pressures, and temperatures are all dimensionless.

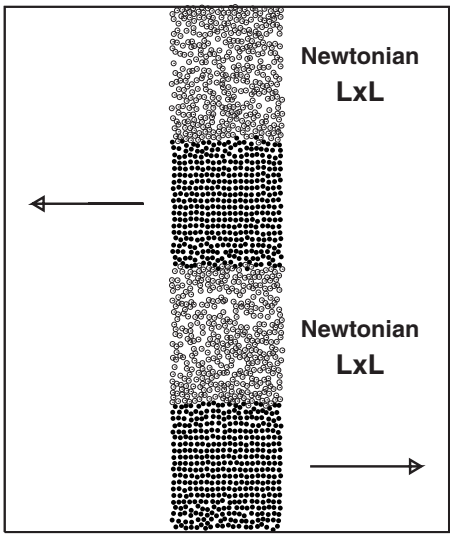

FIG. 2. Two-dimensional version of periodic inhomogeneous boundary-driven shear flow. The system consists of four separate chambers of N particles each. The chambers indicated by arrows are driven to the right and left by moving tether forces. Heat is extracted from the driven chambers to maintain constant internal energy there. The boundary-driven motion of the other two chambers is purely Newtonian.

conditions, just as shown in Fig. 1, but are extended here to three Cartesian space dimensions $\{x,y,z\}$. We take into account the important role of fluctuations in defining local values of the velocity, and the temperature and stress tensors. Section II describes the algorithms, and Sec. III describes the various definitions of temperature for nonequilibrium (as well as equilibrium) systems. Section IV outlines the results of the current simulations. Section V gives the conclusions we have reached as a result of this work. Section VI suggests extensions of this work.

II. SHEAR FLOW ALGORITHMS

Two numerical algorithms, "Sllod" and "Doll's," for spatially periodic shear flow in a volume V both satisfy the macroscopic energy-balance relation $\dot{E}=-\dot{\epsilon}P_{xy}V$. The corresponding solutions differ in effects of order $\dot{\epsilon}^2$, with $P_{xx} > P_{yy}$ in the Sllod case and the reverse using Doll's algorithm. To describe nonequilibrium situations it is natural to introduce the gradients and time derivatives of these variables, with the simplest situations those "stationary states" (necessarily driven by external forces or heat sources) in which all the partial time derivatives (the rates of change at a fixed location) vanish. Steady shear flow can be simulated with homogeneous sources and sinks of momentum and energy through the Doll's and Sllod algorithms. The *adiabatic* versions of these equations of motion (no thermostats or ergostats) introduce an overall flow field imposed with the parameter $\dot{\epsilon}$ through periodic boundary conditions,

$$\dot{x} \equiv (p_x/m) + \dot{\epsilon}y; \quad \dot{y} = (p_y/m) \quad [\text{Sllod or Doll's}].$$

The Sllod algorithm is simply a rewriting of Newton's equations of motion,

$$\ddot{x} = (F_x/m); \quad \ddot{y} = (F_y/m). \tag{102}$$

To see this we introduce the new "momenta" p_x and p_y, (103)

$$p_x \equiv m(\dot{x} - \dot{\epsilon}y); \quad p_y \equiv m\dot{y}. \tag{104}$$

The time derivative of these definitions then gives the Sllod (105) algorithm for $\{\dot{x},\dot{y},\dot{p}_x,\dot{p}_y\}$, (106)

$$\dot{x} = (p_x/m) + \dot{\epsilon}y; \quad \dot{y} = (p_y/m); \tag{107}$$

$$\dot{p}_x \equiv F_x - m\dot{\epsilon}\dot{y} = F_x - \dot{\epsilon}p_y; \quad \dot{p}_y \equiv F_y. \tag{108}$$

In the laboratory frame (where one sees the overall strain rate (109) $\dot{\epsilon}y$ induced by the periodic boundary conditions) p_x and p_y (110) are just $m\dot{x}$ and $m\dot{y}$, and the motion follows from the usual (111) Hamiltonian, (112)

$$\mathcal{H}_{\text{Lab}} = \sum p^2/(2m) + \Phi. \tag{113}$$

If, as in the Sllod algorithm, the momentum (p_x,p_y) is (114) defined instead in the comoving frame then there is no analogous Hamiltonian. To see this in detail suppose that the (116) comoving equations of motion (describing the Newtonian dy- (117) namics) could be derived from a hypothetical comoving (118) Hamiltonian, $\mathcal{H}_{\text{com}}(\{x,y,p_x,p_y\})$, (119)

$$\dot{x} = +(\partial\mathcal{H}_{\text{com}}/\partial p_x) = (p_x/m) + \dot{\epsilon}y, \tag{120}$$

$$\dot{y} = +(\partial\mathcal{H}_{\text{com}}/\partial p_y) = (p_y/m), \tag{121}$$

$$\dot{p}_x = -(\partial\mathcal{H}_{\text{com}}/\partial x) = F_x - \dot{\epsilon}p_y, \quad \dot{p}_y = -(\partial\mathcal{H}_{\text{com}}/\partial y) = F_y. \tag{122}$$

The second partial derivatives of the hypothetical Hamil- (123) tonian with respect to y and p_x should be equal. But we find (124) instead (125)

$$(\partial/\partial y)(\partial\mathcal{H}_{\text{com}}/\partial p_x) = (\partial/\partial y)(\dot{\epsilon}y) = \dot{\epsilon} \tag{126}$$

and (127)

$$(\partial/\partial p_x)(\partial\mathcal{H}_{\text{com}}/\partial y) = (\partial/\partial p_x)(-F_y) = 0, \tag{128}$$

showing that there is no such comoving Hamiltonian. (129)

On the other hand, the very similar Doll's-Tensor equa- (130) tions of motion (which are not Newtonian) do follow from a (131) special Hamiltonian appropriate to the comoving frame, (132)

$$\mathcal{H}_{\text{Doll's}} = \sum p^2/(2m) + \Phi + \dot{\epsilon}\sum yp_x: \tag{133}$$

$$+(\partial\mathcal{H}_{\text{Doll's}}/\partial p_x) = \dot{x} = (p_x/m) + \dot{\epsilon}y; \tag{134}$$

$$+(\partial\mathcal{H}_{\text{Doll's}}/\partial p_y) = \dot{y} = (p_y/m). \tag{135}$$

$$-(\partial\mathcal{H}_{\text{Doll's}}/\partial x) = \dot{p}_x = F_x; \quad -(\partial\mathcal{H}_{\text{Doll's}}/\partial y) = \dot{p}_y = F_y - \dot{\epsilon}p_x. \tag{136}$$

Both the foregoing Sllod and Doll's sets of motion equa- (137) tions are adiabatic, so that the systems they describe heat due (138) to viscous shear as time goes on. Additional time-reversible (139) frictional forces of the form $-\zeta p$ can be added to either set of (140) motion equations to keep the energy or the temperature con- (141) stant [7,8], (142)

$$\{\Delta F = -\zeta p;\ \ p_x \equiv m(\dot{x} - \dot{\epsilon} y);\ \ p_y = m\dot{y};\ \ p_z = m\dot{z}\}.$$

The frictional forces make it possible to explore a spatially homogeneous nonequilibrium steady state with definite values of the (time-averaged) stress and temperature. Both these nonequilibrium properties need proper definitions. We consider several alternative definitions of temperature in Sec. III.

III. DEFINITIONS OF TEMPERATURE

In statistical mechanics a longstanding definition of temperature has been kinetic based on the physical picture of an ideal-gas thermometer [7,9]. Measuring the momenta $\{p\}$ relative to the comoving frame of the kinetic thermometer, the kinetic-theory definition is

$$kT_{xx} \equiv \langle p_x^2/m\rangle; \quad kT_{yy} \equiv \langle p_y^2/m\rangle; \quad kT_{zz} \equiv \langle p_z^2/m\rangle.$$

A simple mechanical model capable of measuring all three temperatures simultaneously is a dilute gas of parallel hard cubes [10].

There is also a configurational analog [11,12],

$$kT_{xx} = \langle F_x^2\rangle/\langle \nabla_x^2 \mathcal{H}\rangle; \quad kT_{yy} = \langle F_y^2\rangle/\langle \nabla_y^2 \mathcal{H}\rangle;$$

$$kT_{zz} = \langle F_z^2\rangle/\langle \nabla_z^2 \mathcal{H}\rangle.$$

The configurational temperature has no clear connection to a physical model of a thermometer but follows instead [11] from a formal integration by parts of the canonical average of $\nabla^2\mathcal{H}$,

$$\langle \nabla^2 \mathcal{H}\rangle \equiv \langle (\nabla \mathcal{H})^2/kT\rangle.$$

Both temperature definitions, kinetic and configurational, have associated ambiguities [1]: fluctuations in the kinetic case and [2] rotation in the configurational case. Consider fluctuations first. The local velocity fluctuates in time. The thermal momentum in the kinetic definition has to be measured in a "comoving" frame. Once the velocity is a local quantity, as well as a time-dependent quantity, its definition becomes crucial. Here we adopt a modification of the "smooth-particle" definition of local velocity [13],

$$v(r) \equiv \sum w(|r - r_i| < h) v_i / \sum w(|r - r_i| < h),$$

where v_i is the velocity of particle i and that particle lies within the range h of the smooth-particle weighting function $w(r<h)$.

Smooth-particle applied mechanics (SPAM) [13] provides spatially very smooth material properties (such as density, velocity, stress, and energy) with two continuous spatial derivatives. The definitions of these properties require a smooth weighting function, $w(r<h)$, which must be continuously twice differentiable, normalized, and which must also have a finite range h. Here we adopt the simplest such weighting function meeting these requirements, Lucy's. In three dimensions Lucy's form for w is

$$w_{\text{Lucy}} = \frac{105}{16\pi h^3}[1 - 6x^2 + 8x^3 - 3x^4]; \quad x \equiv |r|/h;$$

$$\to \int_0^\infty 4\pi r^2 w(r<h)dr \equiv \int_0^h 4\pi r^2 w(r<h)dr \equiv 1.$$

In Sec. IV we show that the smooth particulate velocity fluctuations measured as temperature are best defined through a slight modification of the smooth-particle approach, in which the "self" contributions to the particle sums, Σw and Σwv, are absent. This modification reduces the number dependence inherent in comparing atomistic simulations to continuum predictions.

At first sight, the configurational definition of temperature has an advantage over the kinetic one that a calculation of the stream velocity is not required. But the current work led us to recognize a difficulty in defining configurational temperature away from equilibrium. Consider rotation. Particularly in turbulent flows, *rotation* is important. Although configurational temperature has been touted as a way to avoid defining a local velocity [13], it also contains a small and subtle ambiguity—configurational temperature depends on rotation rate.

A rotating rigid body generates centrifugal forces of order $\omega^2 r$ (offset by tensile forces) at a distance r from the center of mass. The tensile forces contribute to the configurational temperature definition,

$$kT_C \equiv \langle F^2\rangle/\langle \nabla^2 \mathcal{H}\rangle,$$

while the centrifugal ones do not, so that perimeter particles are apparently "hotter" than the cooler interior by (relatively small) contributions of order ω^4.

To see this in a simple two-dimensional example, consider the point (x,y) viewed from an (X,Y) coordinate system rotating counterclockwise at the angular frequency ω,

$$X = x\cos(\omega t) + y\sin(\omega t); \quad Y = y\cos(\omega t) - x\sin(\omega t).$$

Two time differentiations, evaluated at time $t=0$, give the Coriolis, centrifugal (rotating-frame), and centripetal (laboratory-frame) forces,

$$\ddot{X} = \ddot{x} + 2\omega\dot{y} - \omega^2 x = \ddot{x} + 2\omega\dot{Y} + \omega^2 X,$$

$$\ddot{Y} = \ddot{y} - 2\omega\dot{x} - \omega^2 y = \ddot{y} - 2\omega\dot{X} + \omega^2 Y.$$

For rigid rotation at an angular velocity ω a particle at $(x,y)=(r,0)$ with laboratory-frame velocity $(0,\omega r)$ and acceleration $(F_x,0)/m=(-\omega^2 r,0)$, the $\ddot{X}$ equation becomes

$$\ddot{X} = \ddot{x} + 2\omega\dot{y} - \omega^2 x = (F_x/m) + 2\omega^2 r - \omega^2 r \equiv 0 = (F_x/m) + \omega^2 r,$$

showing that the atomistic force (F_x/m) exactly offsets the centrifugal force $\omega^2 r$. Thus the configurational temperature for rigid rotation is proportional to $r^2\omega^4$.

The numerical work described in Sec. IV, for relatively gentle shear flows, supports the view that kinetic temperature is both simpler and better behaved than configurational temperature, with smaller fluctuations in both space and time. In a work still in progress we contrast the two approaches for the problem of a strong shockwave.

IV. SIMULATIONS AND RESULTS

Throughout, we focus on a dense fluid in three space dimensions, with the short-ranged "soft-sphere" potential of Refs. [1,2],

$$\phi(r<1) = 100(1-r^2)^4, \quad \Phi = \sum_{i<j} \phi(|r_{ij}|),$$

where the sum over pairs includes all particle pairs within a distance unity. The total energy of the system consists of a kinetic part in addition to the potential energy Φ,

$$E = K + \Phi, \quad K = \sum p^2/(2m).$$

We focus on the dense-fluid state of Ref. [1], with a density and energy per particle of unity,

$$E/N = Nm/V = N/V = 1,$$

$$6 \times 10^3 = 216 \le N \le 2744 = 14 \times 10^3.$$

Data for homogeneous isoenergetic Doll's and Sllod simulations are given in Ref. [1]] along with complementary results for boundary-thermostated flows. That study showed that the normal-stress differences in the homogeneous simulations are very different from those found in boundary-driven flows. The number dependence in the temperatures and normal-stress differences of the homogeneous flows is nearly negligible, no more than $1/N$ once the number of particles N is a few hundred. By contrast, the boundary-driven temperatures are quite different, as the midstream temperature increases as $N^{2/3}$.

Here we consider in addition *adiabatic deformation* with the Newtonian motion driven by shearing boundary conditions and without any thermostat or ergostat forces. The initial state is a cubic lattice with a kinetic temperature of $kT = 0.01$ and an initial energy per particle of $E = K + \Phi = 0.015N + 0$ (because the nearest-neighbor separation is initially unity just beyond the range of the repulsive forces). We compute and compare two different kinetic temperatures, each with the three components $\{T_{xx}, T_{yy}, T_{zz}\}$. The *time-averaged temperature*, $kT^{\rm TA}$ is

$$kT_{xx}^{\rm TA} \equiv \langle m(\dot{x}_i - \dot{\epsilon} y_i)^2 \rangle,$$

$$kT_{yy}^{\rm TA} \equiv \langle m\dot{y}^2 \rangle,$$

$$kT_{zz}^{\rm TA} \equiv \langle m\dot{z}^2 \rangle,$$

while the instantaneous temperature, $kT^{\rm inst}$, is

$$kT_{xx}^{\rm inst} \equiv \langle m[\dot{x}_i - v_x(r_i,t)]^2 \rangle,$$

$$kT_{yy}^{\rm inst} \equiv \langle m[\dot{y}_i - v_y(r_i,t)]^2 \rangle,$$

$$kT_{zz}^{\rm inst} \equiv \langle m[\dot{z}_i - v_z(r_i,t)]^2 \rangle,$$

where the instantaneous velocity at particle i's location is a modified version of the usual smooth-particle average [13],

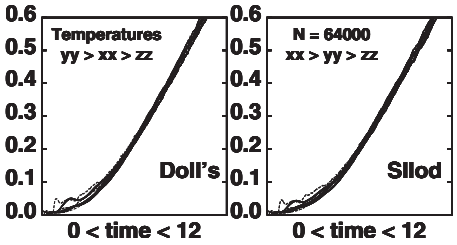

FIG. 3. Overall adiabatic temperature variations for adiabatic-shear flows with $64\times64\times64$ soft spheres with an initial kinetic temperature of 0.01. The strain rate $du_x/dy = \dot{\epsilon}$ is 0.5. $\{T_{xx}, T_{yy}, T_{zz}\}$ are plotted here. For times greater than 3 neither algorithm shows significant differences between the temperatures on the scale of the plots.

$$v(r_i,t) = \sum_{j\neq i} w(r_{ij}) v_j / \sum_{j\neq i} w(r_{ij}).$$

For simplicity we choose Lucy's weight function with the range $h=3$,

$$w(r<h) = \frac{105}{16\pi h^3}(1 - 6x^2 + 8x^3 - 3x^4), \quad x \equiv r/h,$$

for the evaluation of all the smooth-particle sums.

In smooth-particle simulations [13] the "self-terms," in the two particle sums, $w_{ii}v_i$ and w_{ii} are always included. In analyzing equilibrium molecular-dynamics simulations for local velocity fluctuations (the usual kinetic temperature), numerical work shows that there is a much better correspondence with equilibrium temperature when the self-terms are omitted. We have followed that practice here. If the self-terms are included in computing the local stream velocity the resulting kinetic temperatures are roughly 10% lower. With the self-terms omitted the three temperature definitions, time-averaged kinetic, instantaneous kinetic, and configurational, all give similar results.

The need for excluding the "self"-contributions can be rationalized by considering an equilibrium particle i at location r_i with velocity v_i. With its neighbor velocities uncorrelated (as they are at equilibrium within terms of order $1/N$), the smooth-particle velocity at r_i is, on average,

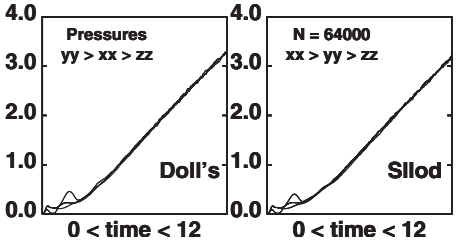

FIG. 4. Overall adiabatic pressure variation for adiabatic-shear flows with $64\times64\times64$ soft spheres with an initial kinetic temperature of 0.01. The strain rate $du_x/dy = \dot{\epsilon}$ is 0.5. $\{P_{xx}, P_{yy}, P_{zz}\}$ are plotted here. For times greater than 3 neither algorithm shows significant differences between the pressures on the scale of the plots.

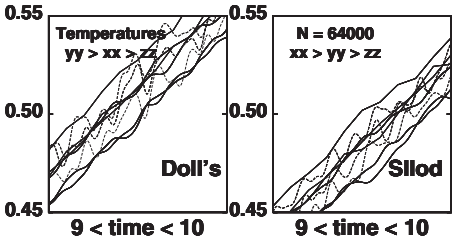

FIG. 5. $\{T_{xx},T_{yy},T_{zz}\}$ are plotted here for portions of 64 000-particle adiabatic simulations of Figs. 3 and 4. The heaviest lines show the laboratory-frame kinetic temperature; the medium lines show kinetic temperature relative to the instantaneous smooth-particle velocity. The light dashed lines show the configurational temperatures, which fluctuate more wildly than the kinetic temperatures. In the steady-state simulations of Ref. [1] the Doll's kinetic temperatures {0.496,0.508,0.493} and the Sllod kinetic temperatures {0.507,0.497,0.493} correspond to an internal per particle energy of exactly unity.

$$v_{\mathrm{SPAM}}(r_i) \equiv \sum_j w_{ij}v_j / \sum_j w_{ij} \simeq w(0)v_i/n, \quad n \equiv N/V,$$

so that the temperature, based on the velocity fluctuations as measured by the differences, $\{v_i - \langle v_{\mathrm{SPAM}}(r_i)\rangle\}$, is reduced by a factor of $[1-w(0)/n]^2$. In the present work the number density n is unity. In accord with this equilibrium argument, we have excluded the "self-terms" in the kinetic parts of the temperatures and pressures illustrated in the figures.

Figures 3 and 4 show the overall increase in temperature and pressure beginning with a homogeneous cubic crystal, at a kinetic temperature of 0.01, and ending at a homogeneous shearing fluid state with a temperature somewhat greater than 0.5. The details of the temperature and pressure for 64 000 particles, in the vicinity of $kT \simeq 0.5$, are shown in Figs. 5 and 6. The fluctuations in the data can be reduced by using even larger systems. Compare Figs. 5 and 6 with the corresponding results for 262 144 particles, shown in Figs. 7 and 8. In these latter simulations the internal energy per particle reaches unity for the Sllod algorithm at a time of 9.799 and for the Doll's algorithm at a time of 9.480.

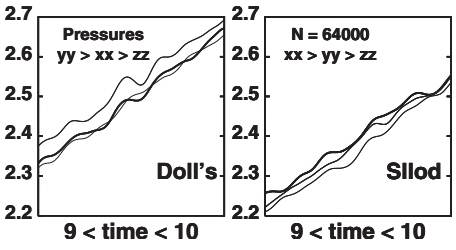

FIG. 6. $\{P_{xx},P_{yy},P_{zz}\}$ are plotted here for portions of the adiabatic simulations of Figs. 3 and 4 (using laboratory-frame kinetic contributions) and correspond to the heavy, medium, and light lines, respectively. In the steady-state simulations of Ref. [1] the Doll's pressures (using laboratory-frame kinetic parts) {2.496,2.528,2.482} and the Sllod pressures {2.516,2.509,2.484} correspond to an internal per particle energy of exactly unity and an average temperature of about 0.5. The shear stress is about the same for the two algorithms, $\sigma_{xy}=0.343$.

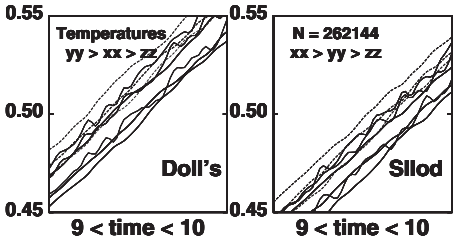

FIG. 7. $\{T_{xx},T_{yy},T_{zz}\}$ are plotted here for portions of 262 144-particle adiabatic-shear simulations. The heaviest lines show the laboratory-frame kinetic temperature; the medium lines show kinetic temperature relative to the instantaneous smooth-particle velocity. The light dashed lines show the configurational temperatures, which fluctuate more than the kinetic temperatures. The kinetic temperatures are nearly the same as those in the stationary shear simulations of Ref. [1].

At a fixed strain rate of 0.5, small-system fluctuations can completely obscure the orderings of $\{T_{ii}\}$ and $\{P_{ii}\}$. By increasing the system size it is possible to verify that the transient fluctuating temperatures and stresses in adiabatic deformation are close to those of the isoenergetic periodic shears, with the orderings $y>x>z$ for Doll's and $x>y>z$ for Sllod. Neither algorithm reproduces the boundary-driven ordering (at the same density, strain rate, and energy) $x>z>y$. We discuss this finding in Sec. V.

V. NONEQUILIBRIUM CONSTITUTIVE RELATIONS

Models for continuum mechanics follow from conservation of mass, momentum, and energy. The differential expressions of these conservation relations are the continuity equation, the equation of motion (which introduces the pressure tensor P as the comoving momentum flux), and the energy equation (which introduces the heat flux vector Q as the comoving energy flux),

$$\dot{\rho} = -\rho\nabla\cdot v; \quad \rho\dot{v} = -\nabla\cdot P; \quad \rho\dot{e} = -\nabla v{:}P - \nabla\cdot Q.$$

The time-and-space-dependent state variables of hydrodynamics are taken from equilibrium thermodynamics, extended to the case in which gradients and time dependence can occur. The state variables at location r and time t are the density, velocity, and energy, $\{\rho(r,t),v(r,t),e(r,t)\}$, and it is assumed that the pressure and heat flux can be defined in

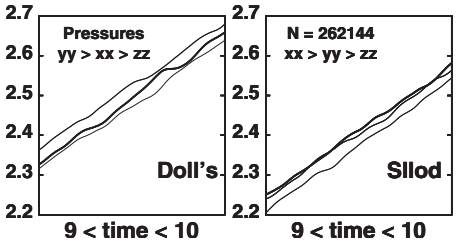

FIG. 8. $\{P_{xx},P_{yy},P_{zz}\}$ are plotted here for portions of 262 144-particle adiabatic-shear simulations and correspond to the heavy, medium, and light lines, respectively. The configurational parts of the pressure are slightly, but significantly, larger than those found in the stationary shear simulations of Ref. [1].

terms of the present values, the gradients, and possibly the past histories of these same variables.

In the present work we have seen that both the temperature (extended from the scalar thermodynamic variable to tensor values) and the stress can differ for two systems with identical densities, strain rates, energies, and constitutive relations (because the underlying particles are the same). Evidently both temperature and stress depend on additional state variables. The relative independence of the normal-stress differences to the system size [1] L suggests that the discrepancy between periodic and boundary-driven systems is insensitive to second derivatives, $\{\nabla\nabla\rho, \nabla\nabla v, \nabla\nabla e\}$, all of which vary as L^{-2}. From the constitutive standpoint it is simplest to imagine a dependence of the normal-stress differences and the temperature tensor on the rate of heating $\dot{e}$. Such a dependence could be used to describe the deviation of the adiabatic transient flows from the corresponding stationary flows. Finding an additional independent constitutive variable to distinguish stationary boundary-driven flows from stationary homogeneous flows is a challenging research goal.

VI. SUMMARY

Evans' emphasis on the exactness of the Sllod algorithm (restricted to adiabatic flows) is confirmed here, as Sllod is nothing but Newton in a different coordinate frame. But it must be noted that the large-system adiabatic pressure tensor exhibits clear differences from the stationary pressure tensor at the same energy, density, and strain rate. Sufficiently large systems, with hundreds of thousands of particles, show that the nonequilibrium temperature tensors of adiabatic transient flows are very similar to those of homogeneous periodic stationary flows. The "realism" of the adiabatic flows is questionable because real boundaries, which normally drive, constrain, and cool flows, are absent. The diffusion time for an N-particle system driven by a strain rate incorporated in its periodic boundary conditions varies as $N^{2/3}$, so that simulation results depend increasingly on their initial conditions as system size increases.

An interesting finding of the present work is that the smooth-particle calculation of local velocity (when that velocity is needed for the computation of the local temperature), $v_{\mathrm{SPAM}}=\Sigma wv/\Sigma w$, is best modified by omitting the self-terms in both sums. In a motionless equilibrium system the "correct" average velocity, about which thermal fluctuations are measured, should vanish. The usual smooth-particle average at particle i, $\langle v_{\mathrm{SPAM}}\rangle$, includes a contribution of order v_i divided by the number of particles included in the sums. For typical useful choices of the weight function and its range h, field variables, such as density and velocity, include contributions from a few dozen particles. When temperature is estimated from fluctuations about a smooth-particle average, omitting the self-terms gives an improved temperature estimate. The improvement is of the order of 10%.

From the constitutive standpoint it is simplest to "explain" the difference between the adiabatic and boundary-driven nonlinear properties through a dependence on $\dot{e}$, where e is the internal energy per unit mass. Though the configurational temperature tensor avoids the problem of defining a local stream velocity, it still includes the effect of rotational contributions, giving rise to "temperature gradients" based on centrifugal forces in the absence of heat flow. Fortunately these rotational temperature contributions are small, of order $\dot{\epsilon}^4$.

VII. WHAT TO DO?

One referee asked us Lenin's famous question with regard to this work's consequences. We hope to stimulate further investigations of microscopic systems from macroscopic points of view. The microscopic analogs of macroscopic temperature, stress, and fluctuations are imperfect but vital in drawing macroscopic conclusions from particle simulations. There is much to do in understanding this correspondence better for more complex systems with rotational and vibrational degrees of freedom. Simulations and theories of elongational flow have led to unresolved controversies as to the "right way" to simulate such flows. See, for instance Refs. [28–36] cited in our Ref. [1]. We believe that the nonlinear aspects of steady deformational flows deserve more study. For unsteady flows even an "exact" algorithm such as Sllod depends on an essential way on the initial conditions unless the deformation rate is very small.

Shockwaves provide more extreme tests of the correspondence between microscopic and macroscopic models. The significance of temperature for quantum systems away from equilibrium needs elucidation too. We are confident that progress along all of these lines can best be achieved by carrying out, analyzing, and comparing series of simulations such as those described in the present work.

ACKNOWLEDGMENTS

We thank Denis Evans for his stimulating comments and Carl Dettmann for his useful remarks on the lack of a Sllod Hamiltonian. We are grateful to the anonymous referees for their constructive criticism.

[1] W. G. Hoover, C. G. Hoover, and J. Petravic, Phys. Rev. E **78**, 046701 (2008).
[2] H. A. Posch and W. G. Hoover, Phys. Rev. A **39**, 2175 (1989).
[3] W. G. Hoover, Lect. Notes Phys. **132**, 373 (1986).
[4] D. J. Evans and G. P. Morriss, Phys. Rev. A **30**, 1528 (1984).
[5] Wm. G. Hoover and W. T. Ashurst, *Theoretical Chemistry, Advances and Perspectives* (Academic, New York, 1975), Vol. 1, p. 1.
[6] D. J. Evans (private communication).
[7] Wm. G. Hoover, *Computational Statistical Mechanics*

(Elsevier, Amsterdam, 1991).
[8] D. J. Evans and G. P. Morriss, *Statistical Mechanics of Nonequilibrium Liquids* (Academic, London, 1990).
[9] W. G. Hoover, B. L. Holian, and H. A. Posch, Phys. Rev. E **48**, 3196 (1993).
[10] W. G. Hoover and A. G. De Rocco, J. Chem. Phys. **36**, 3141 (1962).
[11] L. D. Landau and E. M. Lifshitz, *Statistical Physics* (Mir, Moscow, 1951), Eq. 33.14.
[12] J. Delhommelle, J. Petravic, and Denis J. Evans, Phys. Rev. E **68**, 031201 (2003).
[13] Wm. G. Hoover, *Smooth Particle Applied Mechanics: The State of the Art* (World Scientific, Singapore, 2006).